New lanthanoid biphenolate complexes, their further reactivity with trimethylaluminium and catalytic activity for the polymerisation of *rac*-lactide

Angus C. G. Shephard,[a] Safaa H. Ali,[a] Jun Wang,[a] Zhifang Guo,[a] Murray S. Davies,[a] Glen B. Deacon,[b] Peter C. Junk[a]

[a] College of Science & Engineering, James Cook University, Townsville, QLD. 4811, Australia
[b] School of Chemistry, Monash University, Clayton, Vic, 3800, Australia

Key words: Biphenolate, lanthanoid, aluminium, heterobimetallic, redox transmetallation.

Abstract

A series of rare earth biphenolate complexes of the general form [Ln(mbmp)(mbmpH)(thf)$_3$] (Ln = Y (**1**), Nd (**2**), Gd (**3**), Dy (**4**), Er (**5**), Tm (**6**) and Lu (**7**)) have been synthesised by redox transmetallation/protolysis (RTP) from the free rare earth metal, Hg(C_6F_5)$_2$ and 2,2'-methylenebis(6-*tert*-butyl-4-methylphenol) (mbmpH$_2$). The rare earth metal is six coordinate with one chelating biphenolate mbmp^{2-} ligand and one unidentate monophenolate mbmpH$^-$ ligand. The yttrium complex, when crystallised from hot toluene or deuterated benzene, loses a coordinated thf and exhibits coordination through all three phenolate oxygen atoms, as well as the oxygen of the phenol, yielding two solvates [Y(mbmp)(mbmpH)(thf)$_2$]·*n*solv (solv = PhMe, *n* = 1 (**8a**) or C_6D_6, *n* = 2 (**8b**)). Of these rare earth complexes, the yttrium derivative (**1**) yielded the heterobimetallic complex [AlMe$_2$Y(mbmp)$_2$(thf)$_2$] (**9**) when treated with trimethylaluminium, whereas all other complexes produced the transmetallation product [AlMe(mbmp)(thf)] (**11**). The dinuclear dysprosium complex [Dy$_2$(mbmp)$_3$(thf)$_3$] (**10**) was isolated alongside **11** from the reaction of **4** with trimethylaluminium, suggesting trimethylaluminium instigates a redistribution reaction. The ROP activity of the mononuclear neodymium, dysprosium, lutetium, and aluminium complexes towards *rac*-lactide in toluene at 70 ˚C was found to be poor compared to rare earth complexes of monodentate aryloxides, but increased with increased rare earth ion size.

Introduction

Rare earth alkoxides and aryloxides have been important targets in the development of synthetic methods for reactive rare earth compounds,[1] and complexes of bulky aryloxides are prominent in low coordinate (3-6) rare earth complexes.[1–3] The alkoxides are important in sol gel methods,[1] as feedstocks in MOCVD and ALD deposition of oxide layers,[4] and as catalysts for the ring opening polymerisation of cyclic esters.[5] Of these aryloxides, carbon-bridged biphenolate ligands have seen extensive use over the years in both main group, and transition metal chemistry,[6–9] and more recently, in rare earth chemistry.[10–13] The prevalence of these biphenolate ligands is largely owing to their tunability, their ability to chelate to the metal centre to avoid redistribution reactions, and the catalytic activity of the metal complexes towards the ring opening polymerisation (ROP) of a variety of cyclic esters.[5] Rare earth biphenolate complexes have typically been synthesised by two methods: halide metathesis, or protolysis/ligand exchange.[10–12,14,15] As both methods utilise rare earth halides and alkali metal reagents at some stage in their synthesis, halide or alkali metal inclusion can be observed in the final structure as an undesired consequence.[12] An alternative synthetic approach to rare earth biphenolates, which avoids the potential for halide inclusion or metallate formation, is afforded by redox transmetallation/protolysis

(RTP), utilising the free rare earth metal and bis(pentafluorophenyl)mercury ($Hg(C_6F_5)_2$) as an oxidising agent.[16,17] RTP has become an increasingly popular means of accessing rare earth aryloxides, amides and organometallics, owing to its convenient one pot procedure and the air and moisture stability of the organometallic mercury reagents.[16,17] Several rare earth biphenolates with the general form $[Ln(mbmp)(mbmpH)(thf)_2]$ (Ln = Y, Sm, and Yb), have been synthesised with protolysis/ligand exchange reactions from the corresponding $LnCp_3$ complexes.[11,14] Herein, we describe the synthesis of these heteroleptic rare earth biphenolate complexes, their further reactivity with trimethylaluminium, and their catalytic activity towards the ROP of *rac*-lactide. Both the rare earth biphenolate complexes, and the heterobimetallic biphenolate complexes are expected to be active catalysts for the ROP of *rac*-lactide.

Results and Discussion

Synthesis and Characterisation of Partially Deprotonated Metal Biphenolate Complexes

The RTP reaction of 2,2'-methylenebis(6-*tert*-butyl-4-methylphenol) ($mbmpH_2$) and a range of rare earth metals with $Hg(C_6F_5)_2$ (in a 4:3 (excess):3 mole ratio respectively) gives a heteroleptic trivalent biphenolate complex (Scheme 1) in which one of the $mbmpH_2$ ligands is dianionic ($mbmp^{2-}$) and bidentate, whilst the other is monodentate as it remains protonated at one of the two phenolic sites ($mbmpH^-$), alongside three coordinated thf molecules. This remaining acidic hydrogen can lead to further reactivity with metal alkyls to form heterobimetallic complexes.

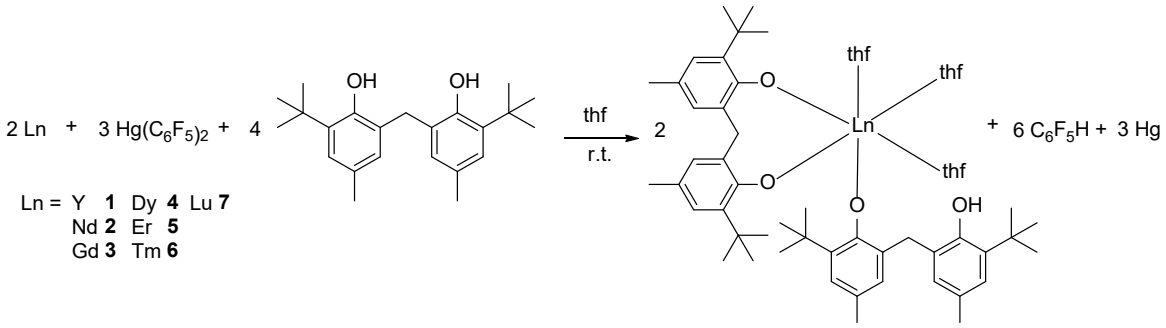

Scheme 1 – RTP reaction of lanthanoid metals with $Hg(C_6F_5)_2$ and $mbmpH_2$

Reactions were carried out in thf at room temperature, with a drop of Hg metal to activate the Ln metal, leading to isolation of complexes **1-7** (Scheme 1) as crystals from concentrated solutions. The yields of complexes **1-7** range from 19 – 92%, which are comparable to previous syntheses of $[Ln(mbmp)(mbmpH)(thf)_2]$, where Ln = Y, Yb, and Sm, synthesised from $LnCp_3$ and $mbmpH_2$ with yields of 34%, 38% (increased to 82% and 87% respectively with a modified workup), and 40% respectively.[11,14] The previous synthesis requires either a prior synthesis of $LnCp_3$ or an extremely expensive commercial purchase. When crystallised from thf, complexes **1-7** are isostructural, with the general form $[Ln(mbmp)(mbmpH)(thf)_3]\cdot n$thf, wherein the dianionic $mbmp^{2-}$ acts as a bidentate ligand, whilst the partially protonated $mbmpH^-$ coordinates only through the phenolate O^- (Figure 1). Single crystals of complex **2** were isomorphous and had unit cell parameters in agreement with complexes **1** and **3-7**, and only connectivity was established. Complexes **1-7** possess a six-coordinate, octahedral Ln core, ligated by one bidentate $mbmp^{2-}$ ligand, O(3) and O(4), in the equatorial sites, one partially deprotonated, monodentate $mbmpH^-$ ligand in an axial position, O(2), and three facially coordinated thf molecules, O(5), O(6) and O(7). The bond angles between bound thf ligands of **1** are (O(5)-Y(1)-O(6) = 89.11(13)°, O(5)-Y(1)-O(7) = 77.66(11)°, and O(6)-Y(1)-O(7) = 77.81(12)° and are

representative of the series. The average Ln-$O_{(Phenolate)}$ bond distances for each complex are in accordance with the reported average bond lengths of [Ln(mbmp)(mbmpH)$(thf)_2$], where Ln = Y, Yb (Average Ln-$O_{(Phenolate)}$ = 2.101 and 2.140 Å respectively),[11] and the decrease in average Ln-O bond length is in accordance with the decrease in ionic radii of the Ln^{3+} centre from **2** to **7** (six coordinate Nd^{3+} = 0.983 Å, and six coordinate Lu^{3+} = 0.861 Å).[18] Selected bond lengths for these partially protonated complexes have been compiled in Table 1.

Complexes **1-7** vary structurally from the previously synthesised biphenolates of yttrium, samarium and ytterbium, ([Ln(mbmp)(mbmpH)$(thf)_2$], Ln = Y, Sm and Yb) where all four oxygen atoms from the two ligands coordinate to the metal centre, one as a coordinated phenol, with two coordinated thf molecules.[11,14] The average Ln – $O_{(Phenolate)}$ bond lengths of **1-7** are in accordance with those of the reported complexes despite despite the structural difference. Moreover, this previous coordination arrangement was achieved by recrystallising complex **1** from a non-coordinating solvent (i.e. toluene or deuterated benzene), resulting in one molecule of thf being displaced by the protonated phenol of $mbmpH^-$ upon heating, yielding complexes **8a/8b** [Y(mbmp)(mbmpH)$(thf)_2$]·*n*solv (solv = PhMe (**8a**) or $2C_6D_6$ (**8b**)) (Figure 2), which are isostructural with the reported complexes.[11] *Further deprotonation does not accompany this step.*

Table 1 - Selected bond lengths (Å) of [Ln(mbmp)(mbmpH)$(thf)_3$] (Ln = Y, Nd, Gd, Dy, Er, Tm, Lu) with average bond lengths italicised.

Bond Lengths (Å)	**1**	**3**	**4**	**5**	**6**	**7**
Ln(1)-O(2)	2.113(3)	2.148(3)	2.130(3)	2.105(3)	2.094(4)	2.080(6)
Ln(1)-O(3)	2.127(3)	2.164(3)	2.144(3)	2.116(3)	2.094(4)	2.101(5)
Ln(1)-O(4)	2.132(3)	2.162(2)	2.144(3)	2.126(3)	2.103(4)	2.099(5)
<Ln(1)-$O_{(Phenolate)}$>	*2.124(5)*	*2.164(5)*	*2.139(5)*	*2.116(5)*	*2.097(7)*	*2.093(9)*
Ln(1)-O(5)	2.430(3)	2.466(3)	2.457(3)	2.415(3)	2.396(5)	2.404(6)
Ln(1)-O(6)	2.402(4)	2.448(3)	2.427(3)	2.399(4)	2.373(4)	2.371(6)
Ln(1)-O(7)	2.445(3)	2.484(3)	2.462(3)	2.433(3)	2.406(4)	2.407(5)
<Ln(1)-$O_{(thf)}$>	*2.426(6)*	*2.466(5)*	*2.449(5)*	*2.416(6)*	*2.392(8)*	*2.394(10)*

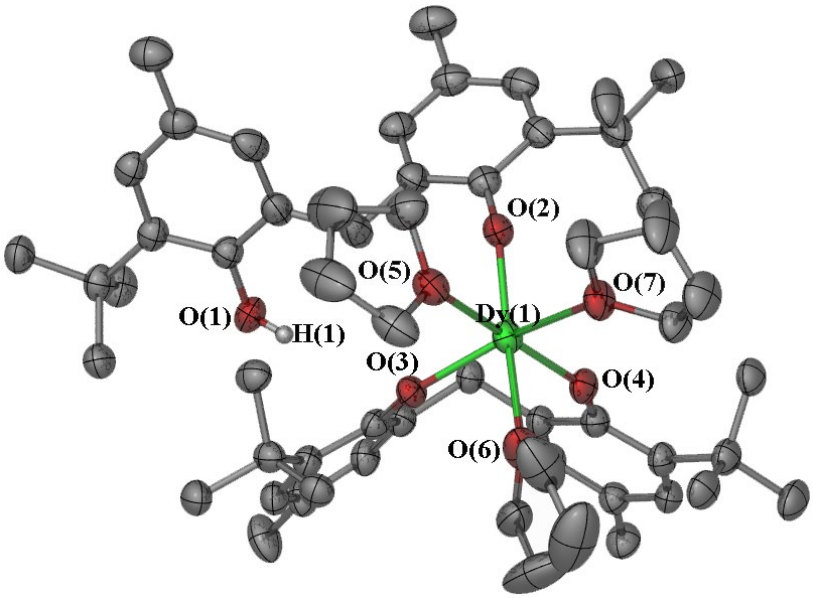

Figure 1 - ORTEP diagram of complex **4** (also representative of **1-3** and **5-7**) showing atom-numbering scheme for relevant atoms. Thermal ellipsoids are drawn at the 50% probability level. Hydrogen atoms and lattice thf are omitted for clarity.

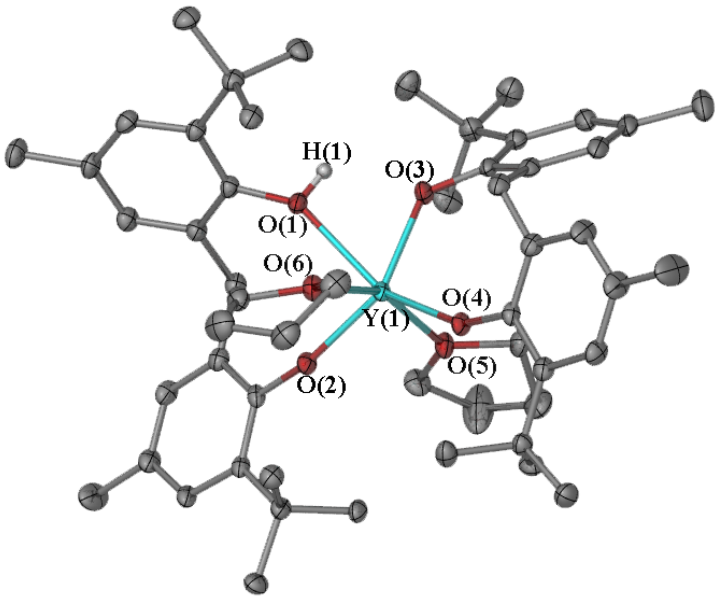

Figure 2 - ORTEP diagram of complex **8a** (also representative of **8b**) showing atom-numbering scheme for relevant atoms. Thermal ellipsoids are drawn at the 50% probability level. Hydrogen atoms and lattice toluene are omitted for clarity.

Complexes **8a** and **8b** are isostructural, varying only in their solvent of crystallisation (toluene and deuterated benzene respectively). Complex **8a** crystallises in triclinic space group *P*-1 with one molecule in the asymmetric unit. Complex **8b** was solved and refined in monoclinic space groups $P2_1/n$ (two molecules in the asymmetric unit) and $C2/c$ (half a molecule in the asymmetric unit) with the latter displaying disorder between phenolic OH and phenolate O, and in the lattice solvent. We present the higher symmetry solution ($C2/c$) herein (see supplementary information for lattice parameters). The complexes have a distorted octahedral yttrium atom, which is chelated by one fully deprotonated $mbmp^{2-}$ and one partially deprotonated $mbmpH^{-}$ in the equatorial positions, and two coordinated thf molecules in the axial positions (O(5)-Y(1)-O(6) = 155.35(7)° (**8a**) and 160.09(9)° (**8b**). Complexes **8a** and **8b** exhibit coordination of the phenolic OH to the metal centre, consistent with the yttrium, samarium and ytterbium biphenolates previously reported.[11,14] O(1) for **8a** and **8b** remains protonated, and the corresponding Y-O(1) bond lengths (2.4106(18) and 2.389(10) Å respectively) are similar to the Y-$O_{(thf)}$ bond lengths (average 2.3714(35) Å) and are considerably longer than the average Y-$O_{(phenolate)}$ (average 2.152(45) Å) for the same complexes.

The IR spectra are consistent with the X-ray crystal structures obtained, showing a single OH stretching frequency at approximately 3510 cm^{-1}. In the spectra of some complexes, partial hydrolysis of the $mbmp^{2-}$ ligands is observed, owing to the high air and moisture sensitivity of the complexes. This resulted in two further OH stretching bands at approximately 3600 cm^{-1} and 3390 cm^{-1}, corresponding to ν(OH) of the free $mbmpH_2$ ligand. In these cases Nujol did not provide adequate protection against hydrolysis during the time to record the IR spectra.

Owing to the paramagnetic nature of many of the complexes, satisfactory ^1H NMR spectra were collected only for the diamagnetic complexes: **1** and **7**. The paramagnetic complexes either produced uninterpretable spectra with significant broadening of signals, or were unable to be recorded at all. Phenolic OH resonances were not observed for **1**, however a broad singlet was observed for the OH resonance in **7**. The phenolate/thf ratios for the

diamagnetic complexes aligned with the corresponding X-ray crystal structures. The extreme sensitivity of the complexes to hydrolysis as described in IR spectra was also evident in the ^{1}H NMR spectra of **1** and **7**.

Elemental analysis was undertaken on each complex after drying under reduced pressure. Variable loss of lattice solvent, and in one case coordinated solvent molecules, was observed. Thus, **1**, **3** and **8b** lost all lattice solvent, **2** lost one lattice thf, **5** lost lattice and two coordinate thf, and **4**, **6**, and **7** retained lattice solvent. In most cases the compositions were supported by complexometric determination of % RE.

Reactivity Towards Trimethylaluminium

As complexes **1-7,** and **8a**/**b** all possess a reactive proton, it was expected that they would exhibit protolysis of trimethylaluminium. This offers a potential source of rare earth-aluminium heterobimetallic biphenolate complexes (e.g. Scheme 2 (a)). Previous attempts to synthesise ytterbium-aluminium heterobimetallics from complexes analogous to **8a**/**8b** and triethylaluminium by this route yielded a discrete ion pair complex $[Yb(mbmp)(thf)_2(dme)][Yb(mbmp)_2(thf)_2]$ rather than a molecular heterobimetallic complex.[11] It has been postulated that coordination of the protonated phenolic OH may have hindered the formation of the molecular heterobimetallic. There is the possibility that the *uncoordinated* phenolic OH of **1** may be more accessible for protolysis.

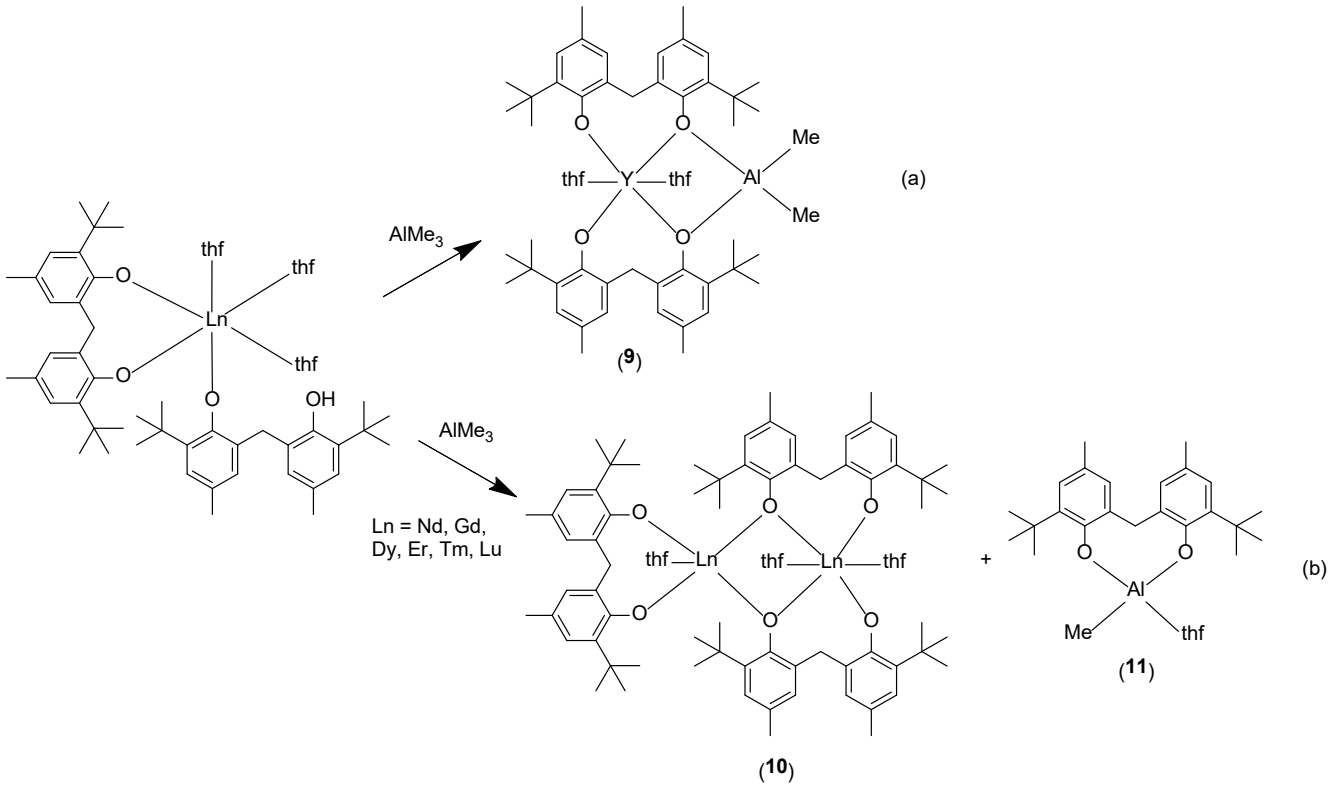

Scheme 2 - Reactions of biphenolate complexes with trimethylaluminium.

Complexes **1-7** were treated with one molar equivalent of trimethylaluminium in toluene at room temperature, yielding either colourless, or orange crystals upon standing at -18 ˚C for several days. Of these reactions, only treatment of complex **1** with trimethylaluminium yielded the targetted heterobimetallic biphenolate complex $[AlMe_2Y(mbmp)_2(thf)_2]$ (**9**) (Scheme 2 (a) and Figure 3). The absence of an OH band at ~3510cm^{-1} in the IR spectrum

of **9** confirmed that protolysis was successfully achieved and a satisfactory microanalysis was obtained.

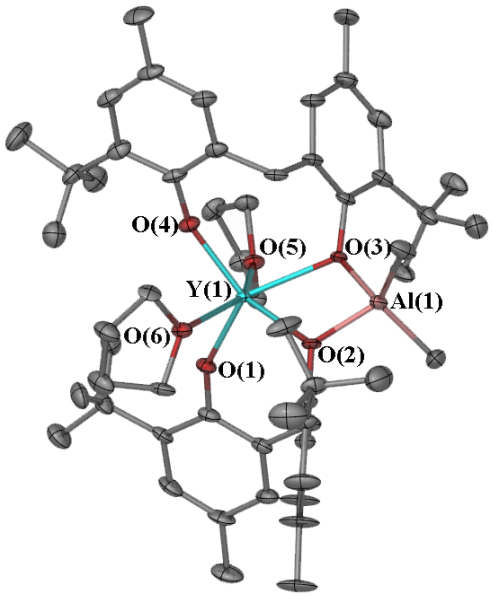

Figure 3 – ORTEP diagram of complex **9** showing atom-numbering scheme for relevant atoms. Thermal ellipsoids are drawn at the 50% probability level. Hydrogen atoms and lattice C_6D_6 are omitted for clarity. Selected bond lengths (Å): Y(1)-O(1) 2.093(3), Y(1)-O(2) 2.375(3), Y(1)-O(3) 2.388(3), Y(1)-O(4) 2.110(3), Y(1)-O(5) 2.399(4), Y(1)-O(6) 2.408(4), Al(1)-O(2) 1.834(4), Al(1)-O(3) 1.827(4).

Complex **9** is comprised of a six-coordinate, distorted octahedral yttrium atom, and a four-coordinate, distorted tetrahedral aluminium atom. Yttrium is ligated by two deprotonated $mbmp^{2-}$ ligands in equatorial positions, and two thf molecules (O(5) and (O6)) in the axial sites ((O(5)-Y(1)-O(6) = 148.70(14)º). One oxygen on both $mbmp^{2-}$ ligands is bound solely to the yttrium (O(1) and O(4)), whilst the other bridges the yttrium and aluminium (O(2) and O(3)). The aluminium is ligated by the two bridging $mbmp^{2-}$ moieties, and two methyl groups. The bridging oxygens of the $mbmp^{2-}$ ligands display considerably longer Y-O bond lengths than their non-bridging counterparts as expected (Figure 3). Complex **9** is isostructural with a reported samarium-aluminium heterobimetallic.[19] The bridging Sm-O bond distances are 2.450 and 2.457 Å, and the bridging O-Al bond distances are 1.836 and 1.839 Å which are consistent with those observed in **9** (Y-O of 2.375 and 2.388 Å, and O-Al of 1.834 and 1.827 Å) in accordance with the difference in ionic radii between Y^{3+} and Sm^{3+}. Lanthanoid-aluminium heterobimetallics have also been reported for N based anilido complexes of both lanthanum and cerium, incorporating a bridging nitrogen in place of oxygen between the two metals.[20]

When complex **4** was treated with trimethylaluminium, two discrete sets of crystals were isolated from the concentrated solution; a dinuclear dysprosium biphenolate complex $[Dy_2(mbmp)_3(thf)_3]$ (**10**) (Figure 4) crystallised as a toluene solvate, and the aluminium complex [AlMe(mbmp)(thf)] (**11**) (Figure 5) crystallised, also as a toluene solvate (Scheme 2 (b)). When complexes **2-7** were treated with trimethylaluminium, the crystalline product was characterised and found to be the aluminium biphenolate complex (**11**), suggesting a similar redistribution occurred, but analogues of **10** could not be crystallised. A similar redistribution has been reported when $[Ln(mbmp)(mbmpH)(thf)_2]$ (Ln = Y and Yb) were treated with diethylzinc, leading to the corresponding zinc biphenolate complex.[11]

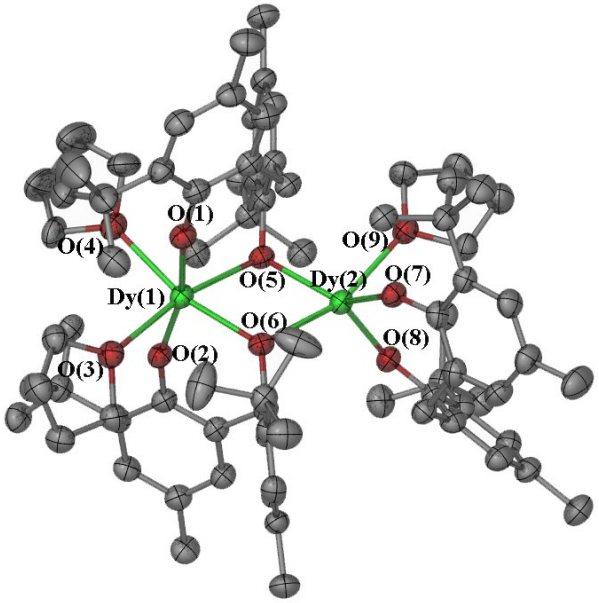

Figure 4 - ORTEP diagram of complex **10** showing atom-numbering scheme for relevant atoms. Thermal ellipsoids are drawn at the 50% probability level. Hydrogen atoms are omitted for clarity. Selected bond lengths (Å): Dy(1)-O(1) 2.173(4), Dy(1)-O(2) 2.170(4), Dy(1)-O(3) 2.415(4), Dy(1)-O(4) 2.424(4), Dy(1)-O(5) 2.361(4), Dy(1)-O(6) 2.296(3), Dy(2)-O(5) 2.311(3), Dy(2)-O(6) 2.340(4), Dy(2)-O(7) 2.094(3), Dy(2)-O(8) 2.105(4), Dy(2)-O(9) 2.426 (4).

Complex **10** is an asymmetrical dinuclear dysprosium complex, and is analogous to a reported lanthanum complex $[La_2(mbmp)_3(thf)_3]$.[11] One dysprosium atom (Dy(1)) is six-coordinate, with a distorted octahedral geometry. There are two bidentate $mbmp^{2-}$ ligands coordinated with one oxygen bound solely to Dy(1) and the other bridging between the two dysprosium atoms, and two thf ligands. The other dysprosium atom (Dy(2)) is five-coordinate, with a distorted square pyramidal geometry, and is coordinated by the two bridging $mbmp^{2-}$ oxygens, a third, terminal $mbmp^{2-}$, and one molecule of thf. The bridging oxygens of the $mbmp^{2-}$ ligands display significantly longer Dy-O bond lengths than their non-bridging counterparts, and Dy(1)-O(1) and Dy(1)-O(2) lengths are significantly longer than Dy(2)-O(7) and Dy(2)-O(8), consistent with the difference in coordination number of the two Dy atoms. However, the Dy-O(thf) bond lengths are little affected. Complex **10** might be viewed as a precursor of a charge separated species, namely $[Dy(mbmp)(thf)_4][Dy(mbmp)_2(thf)_2]$, analogous to a known ytterbium complex.[11]

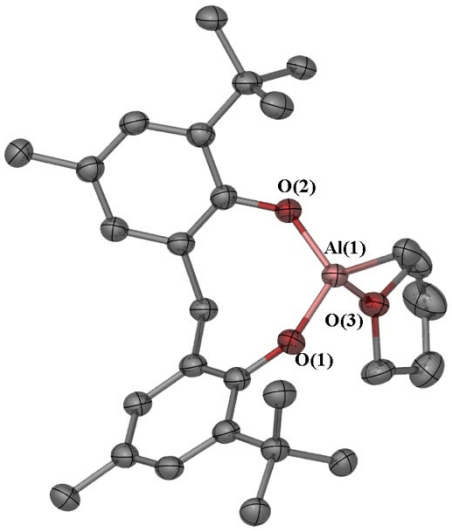

Figure 5 - ORTEP diagram of complex **11** showing atom-numbering scheme for relevant atoms. Thermal ellipsoids are drawn at the 50% probability level. Hydrogen atoms are omitted for clarity. Selected bond lengths (Å): Al(1)-O(1) 1.7118(14), Al(1)-O(2) 1.7253(16), Al(1)-O(3) 1.8851(15).

X-ray and ^{1}H NMR data of **11** isolated, as shown in Scheme 2 (b), and from a direct synthesis in thf (experimental section) were in agreement with reported data for the analogous diethyl ether complex.[21]

Ring Opening Polymerisation Reactions of rac-lactide

A range of rare earth and alkaline earth alkoxide and aryloxide complexes have been shown to be efficient initiators for the ROP of cyclic esters, typically initiating polymerisation at room temperature with reactions progressing to completion within minutes.[5,22–24] These catalysts utilise a Lewis acidic metal centre and undergo polymerisation through a coordination-insertion chain growth mechanism.[22,25–29] The bulky mononuclear biphenolate complexes (**2**, **4**, **7**, and **11**), as well as a mixture of the dinuclear dysprosium and aluminium biphenolate complexes (**10** and **11**), and complex **11** alone, were assessed for ROP initiation of *rac*-lactide. All of the rare earth complexes were found to be catalytically active at 70 ˚C in toluene, but displayed slow reaction rates, poor yields, and high PDIs, while the standalone aluminium complex (**11**) was inactive (Table 2).

Table 2 - Polymerisation of *rac*-lactide initiated by biphenolate complexes[a]

Entry	Initiator	$[M]_0$:[I]	Time (h)	Yield (%)	M_n (g.mol^{-1})[b]	PDI[b]
1	**2**	100	10	75	3653	6.99
2	**4**	100	10	63	2829	3.49
3	**4**	100	20	84	4283	6.62
4	**7**	100	10	30	2644	2.62
5	**10** + **11**	100	10	29	5682	2.52
6	**11**	100	10	0	-	-

[a] Conditions: $[M]_0$ = 0.7 M, solvent: toluene; 70 ˚C.

[b] Measured by GPC against polystyrene standards.

Complex **2** was trialled initially with a 10 hour duration, showing conversion of 75% of monomer to polymer. A similar result was achieved with complex **4** (63% conversion).

Upon extending the reaction duration with complex **4** to 20 hours, an increase in conversion was observed (84% conversion), alongside an increase in PDI, which can be ascribed to transesterification, resulting in lengthened, shortened, or cyclised polymer chains.[30] Notably, the catalytic activity of the complex varied with a change in metal centre, considerably decreasing with a decrease in ionic radius from the larger Nd and Dy complexes, to Lu. This is exhibited by the yield, and the number average molecular weight (M_n) which decreases as ionic radii decrease, but there is also a decrease in PDI, suggesting a more controlled polymerisation. The mixture of **10** and **11** showed very low activity when compared to the mononuclear **4**, likely owing to the reduced accessibility to the dysprosium active sites. However, there was a significant increase in M_n. Complex **11** on its own showed no catalytic activity whatsoever, suggesting that the activity of the mixture is solely dependent on **10**. The lack of reactivity of **11** must be caused by the crowding of Al, which has a much smaller ionic radius than Ln^{3+}. This agrees with the reports that increasing the steric bulk of monodentate phenolate ligands in the *ortho* positions results in reduced performance, caused by hindered access to the metal centre, yielding broad polydispersity indices (PDIs) and large number average molecular weight (M_n) values.[28,31] Similarly, the present carbon bridged biphenolate rare earth complexes showed activity towards ROP initiation of lactide, but with significantly reduced activity for higher steric bulk counterparts, taking significantly longer (>1 hour) to acquire reasonable yields.[12,14]

Despite complexes **2**, **4**, **7**, and **10** displaying ROP initiation capabilities, these bulky biphenolate complexes show significantly lower catalytic efficacy than lower steric bulk, monodentate rare earth aryloxides, requiring considerably longer reaction durations, and exhibiting lower yields and number average molecular weights, and higher polydispersity indices.

Conclusions

In summary, a range of new heteroleptic rare earth biphenolate complexes with the general form [Ln(mbmp)(mbmpH)$(thf)_3$] has been synthesised through RTP reactions, and their further reactivity towards trimethylaluminium, and ROP catalysis capabilities were assessed. Complexes **1**-**7** are isostructural, and consist of a distorted octahedral core, with one chelating $mbmp^{2-}$ ligand, and one partially protonated $mbmpH^{-}$ ligand, bound only throught the phenolate oxygen, and three *fac* thf molecules. Recrystallisation of **1** from toluene or C_6D_6 leads to **8a** and **8b** respectively, with the phenolic oxygen replacing one coordinated thf molecule. **1** was the only rare earth biphenolate complex that reacted with trimethylaluminium to form a heterobimetallic complex (**9**) with a distorted octahedral yttrium atom bridged to a distorted tetrahedral aluminium atom by two $mbmp^{2-}$ ligands. The other rare earth complexes underwent redistribution with trimethylaluminium yielding an aluminium biphenolate complex (**11**) and a dinuclear rare earth biphenolate complex, isolated for dysprosium as **10**, with five and six coordinate dysprosium atoms linked by two bridging $mbmp^{2-}$ ligands. The ROP of *rac*-lactide was studied for selected rare earth complexes. The catalytic activity of the rare earth complexes was found to be much lower than that of previously reported monofunctional aryloxides and decreased as the size of the rare earth ion decreased.

Acknowledgements

ACGS would like to acknowledge the Australian Government's support of this research through an Australian Government Research Training Program scholarship. The authors acknowledge support by the Australian Research Council (DP190100798). Part of this work was conducted using the MX1 beamline at the Australian Synchrotron, which is part of ANSTO.[32]

Experimental

Materials and General Procedures

All manipulations were performed under nitrogen, using standard Schlenk techniques. Solvents (thf and toluene) were distilled from sodium benzophenone before use. 2,2'-Methylene-bis(6-*tert*-butyl-4-methylphenol), trimethylaluminium, and *rac*-lactide were commercially available, and used without further purification. Bis(pentafluorophenyl)mercury was prepared by the literature method.[33] Metal analyses were determined by Na_2H_2edta titration with a Xylenol Orange indicator and hexamethylenetetramine buffer, after decomposition of complexes with dilute HCl. For the heterobimetallic complex (**9**), aluminium was masked in this process by addition of 5% sulfosalicylic acid solution.[34] Infrared spectra (4000–400 cm^{-1}) were obtained as Nujol mulls between NaCl plates with a Nicolet-Nexus FT-IR spectrometer. ^{1}H-NMR spectra were recorded on a Bruker 400 MHz spectrometer. The chemical shifts were referenced to residual solvent peaks. Molecular weights and molecular weight distributions were determined against polystyrene standards by gel permeation chromatography (GPC) on a 1260 Infinity II Multi-Detector GPC (Agilent Technologies) equipped with an ultraviolet (UV) absorbance and refractive index detector. The two PLgel 5 µL MIXED-C columns (300 x 7.5 mm) (Agilent Technologies) were calibrated using polystyrene narrow standards in thf at 35 ˚C, and using thf (HPLC grade) as an eluent with a flow rate of 1.0 mL/min at 35 ˚C. Crystal data and refinement details are given in **Table S1**. CCDC 2099577 for compound **1**, 2099579-2099583 for compound **3-7**, CCDC 2099584 for compound **8a**, CCDC 2099585 for compound **8b**, CCDC 2099586-2099588 for compound **9-11**, contain the supplementary crystallographic data for this paper. These data can be obtained free of charge from The Cambridge Crystallographic Data Centre via www.ccdc.cam.ac.uk/data_request/cif.

Syntheses

[Y(mbmp)(mbmpH)(thf)$_3$]·3thf (1)

A Schlenk flask equipped with a magnetic stirrer bar was charged with mbmpH_2 (1.36g; 4.00 mmol), Hg(C_6F_5)$_2$ (1.60 g; 3.00 mmol), one drop of Hg metal (to form a reactive lanthanoid-mercury amalgam) and excess yttrium filings (0.27 g; 3.0 mmol). Anhydrous thf (~20 mL) was added by cannula, and the reaction mixture stirred at room temperature for 3 days. Excess yttrium metal and mercury were allowed to settle before isolating the supernatant liquid by a filtration cannula. The resulting filtrate was concentrated under reduced pressure to ~10 mL and allowed to stand at room temperature to crystallise, yielding small, pale brown crystals (1.80 g, 92%). *Anal.* Calc. for $C_{58}H_{85}O_7Y$ (983.19g.mol^{-1} after loss of three lattice thf): C, 70.85; H, 8.71; Y, 9.04. Found: C, 70.43; H, 8.20; Y, 8.76%. ^{1}H-NMR (400 MHz, C_6D_6, 25 ˚C): δ 7.40 (d, 4H, Ar), 7.16 (d, 4H, Ar), 3.73 (s, 4H, CH_2), 3.57 (m, 24H, thf), 2.28 (s, 12H, $ArCH_3$), 1.57 (s, 36H, $C(CH_3)_3$), 1.31 (s, 24H, thf). IR (Nujol, cm^{-1}): 3501 s, 1960 w, 1887 w, 1740 s, 1568 s, 1254 w, 1070 m, 1012 m, 914 s, 861 m, 792 w, 726 m, 669 s.

[Nd(mbmp)(mbmpH)(thf)$_3$]·3thf (2)

The synthesis of complex **2** was carried out in the same way as that described for complex **1**, but neodymium filings (0.43 g; 3.0 mmol) were used in place of yttrium. Blue-green crystals were obtained from ~10 mL of thf at 4 ˚C (1.20 g, 51%). *Anal.* Calc. for $C_{66}H_{101}O_9Nd$ (1182.74g.mol^{-1} after loss of one lattice thf): C, 67.02; H, 8.61; Nd, 12.20. Found: C, 66.05; H, 8.43; Nd, 12.08%. IR (Nujol, cm^{-1}): 3509 s, 1966 w, 1742 m, 1603 s, 1562 w, 1532 w, 1459 m, 1378 m, 1161 m, 1069 m, 1023 m, 862 m, 818 m, 794 m, 752 w, 723 w, 668 m.

[Gd(mbmp)(mbmpH)(thf)$_3$]·3thf (3)

The synthesis of complex **3** was carried out in the same way as that described for complex **1**, but gadolinium powder (0.48 g; 3.0 mmol) was used in place of yttrium. Brown crystals were obtained from ~10 mL of thf at -18 ˚C (0.40g, 19%). *Anal.* Calc. for $C_{58}H_{85}O_7Gd$ (1051.54 g.mol^{-1} after loss of three lattice thf): C, 66.25; H, 8.15; Gd, 14.95. Found: C, 65.87; H, 7.95; Gd, 14.80%. IR (Nujol, cm^{-1}): 3505 s, 1744 m, 1712 w, 1645 s, 1604 m, 1533 w, 1509 m, 1456 m, 1378 m, 1262 m, 1179 m, 1072 m, 955 m, 941 m, 913 m, 862 m, 820 m, 718 m, 672 m.

[Dy(mbmp)(mbmpH)(thf)$_3$]·3thf (4)

The synthesis of complex **4** was carried out in the same way as that described for complex **1**, but dysprosium powder (0.49 g, 3 mmol) was used in place of yttrium. Dark yellow crystals were obtained from ~10 mL of thf at 4 ˚C (1.87 g, 70%). *Anal.* Calc. for $C_{70}H_{109}O_{10}Dy$ (1273.10g.mol^{-1}): C, 66.04; H, 8.63; Dy, 12.76. Found: C, 66.07; H, 8.92%. IR (Nujol, cm^{-1}): 3508 s, 1741 m, 1604 s, 1560 w, 1533 w, 1463 m, 1378 m, 1263 m, 1212 m, 1161 m, 1070 m, 1019 m, 956 w, 913 m, 863 m, 820 m, 794 m, 770 m, 723 w, 669 m.

[Er(mbmp)(mbmpH)(thf)$_3$]·3thf (5)

The synthesis of complex **5** was carried out in the same way as that described for complex **1**, but erbium powder (0.50 g, 3 mmol) was used in place of yttrium. Orange crystals were obtained from ~10 mL of thf at 4 ˚C (0.53g, 29%). *Anal.* Calc. for $C_{50}H_{69}O_5Er$ (917.34 g.mol^{-1} after loss of two thf of solvation and three lattice thf): C, 65.46; H, 7.58; Er, 18.23. Found: C, 65.11; H, 7.19; Er, 18.02%. IR (Nujol, cm^{-1}): 3509 s, 1740 m, 1713 w, 1607 s, 1560 m, 1370 m, 1262 m, 1069 m, 965 m, 861 m, 810 m.

[Tm(mbmp)(mbmpH)(thf)$_3$]·3thf (6)

The synthesis of complex **6** was carried out in the same way as that described for complex **1**, but thulium filings (0.51 g, 3 mmol) were used in place of yttrium. Green crystals were obtained from ~10 mL of thf at -18 ˚C (0.69 g, 25%) *Anal.* Calc. for $C_{70}H_{109}O_{10}Tm$ (1279.54g.mol^{-1}): C, 65.71; H, 8.59; Tm, 13.20. Found: C, 65.86; H, 8.67; Tm, 12.53%. IR (Nujol, cm^{-1}): 3508 s, 1741 m, 1639 s, 1604 s, 1548 w, 1532 m, 1166, m, 1045 m, 967 m, 857 m, 770 m, 752 m, 718 w 670 m.

[Lu(mbmp)(mbmpH)(thf)$_3$]·3thf (7)

The synthesis of complex **6** was carried out in the same way as that described for complex **1**, but lutetium filings (0.53 g, 3 mmol) were used in place of yttrium. Pale brown crystals were obtained from ~10 mL of thf at 4 ˚C (1.75 g, 68%) *Anal.* Calc. for $C_{70}H_{109}O_{10}Lu$ (1285.57g.mol^{-1}): C, 65.40; H, 8.55. Found: C, 65.27; H, 8.38; .^{1}H-NMR (400 MHz, C_6D_6, 25 ˚C): δ 7.34 (s, 4H, Ar), 7.18 (s, 4H, Ar), 5.75 (br s, 1H, ArOH), 3.98 (s, 4H, CH_2) 3.60 (s, 24H, thf), 2.28 (s, 12H, $ArCH_3$), 1.59 (s, 36H, $C(CH_3)_3$), 1.34 (s, 24H, thf). IR (Nujol,

cm^{-1}): 3506 s, 1743 m, 1638 s, 1604 s, 1532 m, 1509 m, 1444 m, 1370 m, 1266 m, 1073 m, 1019 m, 967 m, 914 m, 862 m, 822 m, 795 m, 769 m, 722 m, 674 w, 613 w.

[Y(mbmp)(mbmph)(thf)$_2$]·PhMe (8a)

The synthesis of complex **8a** was carried out in the same way as that described for complex **1**, but, after filtration, all solvent was removed under vacuum, and the residue recrystallised by slow cooling of a hot toluene solution (~10 mL) giving single crystals of **8a**.

[Y(mbmp)(mbmpH)(thf)$_2$]·2C$_6$D$_6$ (8b)

The synthesis of complex **8b** was carried out in the same was as that described for complex **8a**, but **8b** was a result of recrystallising from hot deuterated benzene. *Anal.* Calc. for $C_{54}H_{77}O_6Y$ (911.09 g.mol^{-1} after loss of two lattice C_6D_6): C, 71.19; H, 8.52; Y, 9.76. Found: C, 70.83; H, 8.13; Y, 9.37%.

[AlMe$_2$Y(mbmp)$_2$(thf)$_2$]·2C$_6$D$_6$ (9)

A Schlenk flask was charged with **1** (1.80 g, 1.8 mmol) and dissolved in anhydrous toluene (~10 mL), and a 2.0 M solution of trimethylaluminium in toluene (0.90 mL, 1.8 mmol) was added at room temperature. The solution was cooled to -18 ˚C, and small crystals unsuitable for X-ray analysis were obtained. The supernatant solution was removed by filtration, and the crystalline material was dried under reduced pressure, and recrystallised from hot deuterated benzene yielding colourless crystals (0.45 g, 22%). *Anal.* Calc. for $C_{56}H_{82}AlO_6Y$ (967.13 g.mol^{-1} after loss of two lattice C_6D_6): C, 69.55; H, 8.55; Y, 9.19. Found: C, 69.22; H, 8.33; Y, 9.03%. ^{1}H NMR (400 MHz, C_6D_6, 25 ˚C): δ = 7.26 (d, 4H, Ar, *J* = 2.1 Hz), 7.15 (d, 4H, Ar, *J* = 2.1 Hz), 4.18 (d, 2H, CH_2, *J* = 13.7 Hz), 3.68 (d, 2H, CH_2 *J* = 13.7 Hz), 3.58 (m, 24H, thf), 2.27 (s, 12H, $ArCH_3$), 1.60 (s, 36H, $C(CH_3)_3$), 1.21 (m, 24H, thf), -0.28 (s, 6H, $AlCH_3$). Although the NMR sample contained an excess of thf, it establishes the mbmp:Me ratio. IR (Nujol, cm^{-1}): 2725 w, 2369 w, 2214 w, 1891 m, 1740 s, 1605 s, 1258 w, 1012 w, 800 w, 722 m, 669 m, 587 m, 518 m.

[Dy$_2$(mbmp)$_3$(thf)$_3$]·2PhMe (10)

The synthesis of complex **10** was carried out in the same way as that described for complex **9**, but complex **4** (1.87 g, 1.4 mmol) was used in place of complex **1**, and a 2.0 M solution of trimethylaluminium in toluene (0.70 mL, 1.4 mmol) was added. Amber crystals suitable for X-ray analysis were obtained from the toluene solution at -18 ˚C, alongside crystals of **10**. As **10** and **11** were obtained as a mixture, discrete spectroscopic and elemental analysis was not able to be obtained.

[AlMe(mbmp)(thf)]·PhMe (11)

Method A: A Schlenk flask was charged with **2**-**6** (1 equivalent) and dissolved in anhydrous toluene (~10 mL), and a 2.0 M solution of trimethylaluminium in toluene (1 equivalent) was added at room temperature. The solution was cooled to -18 ˚C, and colourless crystals of **11** were obtained and were identified by X-ray crystallography.

Method B: A Schlenk flask equipped with a magnetic stirrer bar was charged with mbmpH$_2$ (0.89 g, 2.6 mmol) and dissolved in anhydrous thf (~30 mL). The solution was cooled to 0 ˚C, and a 2.0 M solution of trimethylaluminium in toluene (1.2 mL, 2.4 mmol) was added dropwise. The resulting solution was allowed to warm to room temperature, and was stirred for 3 hours before removing the solvent under reduced pressure. The solids were resuspended in anhydrous toluene, and the solution removed by filter cannula. Yellow/orange crystals were obtained from the solution at -18 ˚C (0.44 g, 45%). *Anal.* Calc. for $C_{28}H_{41}O_3Al$ (452.60g.mol^{-1} after loss of one lattice toluene): C, 74.30; H, 9.13. Found:

C, 74.12; H, 8.95%. ^{1}H NMR (400 MHz, C_6D_6, 25 ˚C): δ = 7.27 (d, 2H, Ar, *J* = 1.9 Hz), 7.14 (d, 2H, Ar, *J* = 1.9 Hz), 4.22 (d, 1H, CH_2, *J* = 13.7 Hz), 3.58 (d, 1H, *J* = 13.7 Hz) 3.53 (m, 4H, thf), 2.27 (s, 6H, $ArCH_3$), 1.60 (s, 18H, $C(CH_3)_3$), 0.95 (m, 4H, thf), -0.28 (s, 3H, $AlCH_3$). IR (Nujol, cm^{-1}): 2377 m, 2214 w, 2054 w, 1940 w, 1854 m, 1744 m, 1638 s, 1462 m, 1255 m, 1074 s, 955 m, 804 w, 722 s.

Crystal and refinement data

Single crystals covered with viscous hydrocarbon oil were mounted on a glass fibre. Data were obtained at -173 ˚C (100 K) on the MX1: Macromolecular Crystallography beamline at the Australian Synchrotron, Victoria, Australia. Data collection and integration on the MX1: Macromolecular Crystallography beamline was accomplished using Blu-Ice.[35] The structures were solved using SHELXS7 and refined by full-matrix least-squares on all F2 data using SHELX2014[36] in conjunction with the X-Seed graphical user interface.[37] All hydrogen atoms were placed in calculated positions using the riding model. Data collection and refinement details are collated in the SI (Table S1) and selected bond lengths for compounds **1**, and **3-7** are in Table 1. The unit cell of complex **2** was determined and found to be isostructural with complex **1** and **3-7**, but data collected from the X-ray experiment was poor, and only unit cell data is included to show it is isostructural with these compounds Complex **8b** was initially solved and refined in monoclinic space group $P2_1/n$ with two molecules in the asymmetric unit, where the phenolic and phenolate functional groups displayed no disorder. We then detected higher symmetry and solved and refined the structure in monoclinic space group $C2/c$ with half a molecule in the asymmetric unit and having disorder between phenolic OH and phenolate O, and in the lattice solvent (C_6D_6). In this paper we present the higher symmetry solution ($C2/c$) (see supplementary information for lattice parameters).

Typical procedure for polymerisation reactions

A Schlenk flask equipped with a magnetic stirrer bar was charged with *rac*-lactide (0.20 g, 1.39 mmol) and anhydrous toluene (1.5 mL). The contents of the flask were heated to 70 ˚C with stirring, and the initiator (**2, 4, 7**, **10** + **11**, or **11**) (1.39×10^{-2} mmol) in anhydrous toluene (0.5 mL) was added slowly by syringe. The solution was stirred for 10 hours and then quenched with ethanol (2 mL) and concentrated hydrochloric acid (2-3 drops), before being poured into hexanes (40 mL) to precipitate the polymer. The suspension was filtered, and the polymer dried in a vacuum oven at 40 ˚C to remove residual solvent.

As complexes **1-7** are isostructural, catalytic studies were undertaken on metal centres that represented a range of relative ionic radii: large (Nd = **2**), medium (Dy = **4**), and small (Lu = **7**).

References

1 D. C. Bradley, R. C. Mehrotra, I. P. Rothwell and A. Singh, *Alkoxo and Aryloxo Derivatives of Metals*, Academic Press, London, 2001.

2 T. J. Boyle and L. A. M. Ottley, *Chem. Rev.*, 2008, **108**, 1896–1917.

3 F. Ortu and D. P. Mills, *Handbook on the Physics and Chemistry of rare earths*, 55th edn., 2019.

4 H. C. Aspinall, J. F. Bickley, J. M. Gaskell, A. C. Jones, G. Labat, P. R. Chalker and P. A. Williams, *Inorg. Chem.*, 2007, **46**, 5852–5860.

5 D. M. Lyubov, A. O. Tolpygin and A. A. Trifonov, *Coord. Chem. Rev.*, 2019, **392**, 83–145.

6 J. Wu, T. L. Yu, C. T. Chen and C. C. Lin, *Coord. Chem. Rev.*, 2006, **250**, 602–626.

7 A. van der Linden, C. J. Schaverien, N. Meijboom, C. Ganter and A. G. Orpen, *J. Am. Chem. Soc.*, 1995, **117**, 3008–3021.

8 F. G. Sernetz, R. Mülhaupt, F. Amor, T. Eberle and J. Okuda, *J. Polym. Sci. Part A Polym. Chem.*, 1997, **35**, 1571–1578.

9 M. H. Chisholm, J. H. Huang, J. C. Huffman, W. E. Streib and D. Tiedtke, *Polyhedron*, 1997, **16**, 2941–2949.

10 M. Deng, Y. Yao, Q. Shen, Y. Zhang and J. Sun, *Dalton Trans.*, 2004, **4**, 944–950.

11 R. Qi, B. Liu, X. Xu, Z. Yang, Y. Yao, Y. Zhang and Q. Shen, *Dalton Trans.*, 2008, **7**, 5016–5024.

12 Z. Liang, X. Ni, X. Li and Z. Shen, *Inorg. Chem. Commun.*, 2011, **14**, 1948–1951.

13 B. D. Mahoney, N. A. Piro, P. J. Carroll and E. J. Schelter, *Inorg. Chem.*, 2013, **52**, 5970–5977.

14 Y.-F. Tan, X.-P. Xu, K. Guo, Y.-M. Yao, Y. Zhang and Q. Shen, *Polyhedron*, 2013, **61**, 218–224.

15 L. Bao, Y. Yingming, D. Mingyu, Z. Yong and S. Qi, *J. Rare Earths*, 2006, **24**, 264–267.

16 G. B. Deacon, C. M. Forsyth and S. Nickel, *J. Organomet. Chem.*, 2002, **647**, 50–60.

17 Z. Guo, R. Huo, Y. Q. Tan, V. Blair, G. B. Deacon and P. C. Junk, *Coord. Chem. Rev.*, 2020, **415**, 213232.

18 R. D. Shannon, *Acta Crystallogr. Sect. A*, 1976, **32**, 751–767.

19 I. Korobkov and S. Gambarotta, *Organometallics*, 2009, **28**, 4009.

20 R. Thim, D. Schädle, C. Maichle-Mössmer and R. Anwander, *Chem. – A Eur. J.*, 2019, **25**, 507–511.

21 B. T. Ko, Y. C. Chao and C. C. Lin, *Inorg. Chem.*, 2000, **39**, 1463–1469.

22 R. H. Platel, L. M. Hodgson and C. K. Williams, *Polym. Rev.*, 2008, **48**, 11–63.

23 L. Clark, G. B. Deacon, C. M. Forsyth, P. C. Junk, P. Mountford and J. P. Townley, *Dalton Trans.*, 2010, **39**, 6693–6704.

24 L. Clark, G. B. Deacon, C. M. Forsyth, P. C. Junk, P. Mountford, J. P. Townley and J. Wang, *Dalton Trans.*, 2013, **42**, 9294–9312.

25 B. J. O'Keefe, M. A. Hillmyer and W. B. Tolman, *J. Chem. Soc., Dalton. Trans.*, 2001, 2215–2224.

26 O. Dechy-Cabaret, B. Martin-Vaca and D. Bourissou, *Chem. Rev.*, 2004, **104**, 6147–6176.

27 S. Agarwal, C. Mast, K. Dehnicke and A. Greiner, *Macromol. Rapid Commun.*, 2000, **21**, 195–212.

28 I. Palard, M. Schappacher, A. Soum and S. M. Guillaume, *Polym. Int.*, 2006, **55**, 1132–1137.

29 A. Amgoune, C. M. Thomas and J. F. Carpentier, *Pure Appl. Chem.*, 2007, **79**, 2013–2030.

30 W. J. Evans and H. Katsumata, *Macromolecules*, 1994, **27**, 2330–2332.

31 W. M. Stevels, M. J. K. Ankoné, P. J. Dijkstra and J. Feijen, *Macromolecules*, 1996, **29**, 6132–6138.

32 N. P. Cowieson, D. Aragao, M. Clift, D. J. Ericsson, C. Gee, S. J. Harrop, N. Mudie, S. Panjikar, J. R. Price, A. Riboldi-Tunnicliffe, R. Williamson and T. Caradoc-Davies, *J. Synchrotron Radiat.*, 2015, **22**, 187–190.

33 F. T. Edelmann, in *Lanthanides and Actinides*, ed. W. A. Herrmann, Thieme, Stuttgart, Volume 6., 1997, vol. 6, pp. 48–49.

34 G. Schwarzenbach and H. Flashka, *Complexometric Titrations*, Methuen, London, 2nd edn., 1969.

35 T. M. McPhillips, S. E. McPhillips, H. J. Chiu, A. E. Cohen, A. M. Deacon, P. J. Ellis, E. Garman, A. Gonzalez, N. K. Sauter, R. P. Phizackerley, S. M. Soltis and P. Kuhn, *J. Synchrotron Radiat.*, 2002, **9**, 401–406.

36 G. M. Sheldrick, *Acta Crystallogr. Sect. C Struct. Chem.*, 2015, **71**, 3–8.

37 L. J. Barbour, *J. Supramol. Chem.*, 2001, **1**, 189–191.